Acta Physica Polonica B Proceedings Supplement **17**, 7-A2 (2024)

CLASSIFICATION OF SIGNAL EVENTS FOR CPT SYMMETRY STUDIES WITH J-PET USING MACHINE LEARNING TECHNIQUES*

N. Chug†, P. Moskal

on behalf of the J-PET Collaboration

Faculty of Physics, Astronomy, and Applied Computer Science
Jagiellonian University, Kraków, Poland
and
Center for Theranostics, Jagiellonian University, Kraków, Poland

Received 7 October 2024, accepted 28 October 2024,
published online 27 November 2024

The deviations from combined Charge, Parity, and Time (CPT) symmetry could indicate the presence of new physics beyond the current theoretical framework. The positronium (Ps), the lightest bound state of an electron–positron pair, offers a unique probe for such investigations because it is an eigenstate of charge conjugation (C) and parity (P). This work explores the potential of the Jagiellonian Positron Emission Tomography (J-PET) detector for sensitive tests of CPT symmetry in the three-photon decay of ortho-Ps (o-Ps) atom. The CPT symmetry invariance in o-Ps decays has been previously tested using the J-PET detector, measuring the CPT-violating angular correlation between the o-Ps spin and its annihilation photon momenta, achieving a precision of 0.00067 ± 0.00095. However, a range of five orders of magnitude is still unexplored to test its exactness. A Monte Carlo simulation study is presented to distinguish between the o-Ps signal and background events using Multivariate Data Analysis (TMVA). We discuss the impact of improving the sample purity in enhancing the sensitivity of the CPT symmetry test.

DOI:10.5506/APhysPolBSupp.17.7-A2

1. Introduction

The precise validation of fundamental symmetries, such as CPT, is essential to comprehend the universe. While CPT is widely regarded as an exact symmetry, ongoing experimental investigations continue to scrutinize

* Presented at the 5th Jagiellonian Symposium on *Advances in Particle Physics and Medicine*, Cracow, Poland, June 29–July 7, 2024.

† Corresponding author: `neha.chug@doctoral.uj.edu.pl`

for potential violations, especially within systems involving charged leptons like positronium [1, 2]. The positronium, a bound state of an electron and a positron, offers a unique platform for such studies [3, 4]. Previous experiments utilizing detectors such as Gammasphere [5] and J-PET [6] have established stringent constraints on CPT invariance, but further advancements in experimental techniques are imperative to achieve even higher precision levels [7–9]. The experiments have tested the exactness of CPT symmetry in electromagnetic interactions through the 3γ decays of polarized positronium atoms. The CPT-odd angular correlation operator, defined as $\vec{S} \cdot (\vec{k}_1 \times \vec{k}_2)$, between the spin of ortho-positronium (o-Ps) and normal to the decay plane of its annihilation photons, is studied. The three annihilation photons from the o-Ps decay are co-planar. A non-zero expectation value of this operator would indicate a signature of CPT symmetry violation [10].

The present work aims at improving further the precision limit of the testing of the CPT-odd operator using the J-PET detector [11–13]. It is a versatile detector from plastic scintillators optimized for recording photons emitted from annihilations of e^+e^- or via the formation of positronium atoms [14–18]. The paper describes the methodology employed to distinguish the ortho-positronium signal events from the background using machine learning classification methods to evaluate the CPT-odd operator. The results are compared to the traditional cut-based approach for identifying signal events.

2. Method

The Multivariate Analysis is used to select the signal events in evaluating the CPT-odd angular correlation operator with the J-PET detector. The boosted decision trees (BDT) and multilayer perceptrons (MLP) neural network methods from the Toolkit for Multivariate Analysis (TMVA) [19, 20] are utilized to explore the possibility of improving the signal significance. The algorithms are used in the perspective of separating the o-Ps signal from the background events.

We use a Monte Carlo simulated sample prepared in the framework of the J-PET detector [21] for event classification using BDT and MLP algorithms. The event for this study is defined as three Compton scattered interactions of photons in the plastic scintillators of the detector, which includes the primary and the secondary Compton scatterings. It is a 12-fold event corresponding to every photon's interaction position (X, Y, Z) and time (t) in the detector [22]. The signal event consists of three annihilation photons from the o-Ps decay, while the other 3γ events that mimic the signal are the background. A pre-selection condition on energy deposited by a single photon in an event within the range of 30–340 keV was applied while preprocessing the data before using any classification algorithm.

The input variables used for the TMVA neural networks and boosted decision trees were derived from mathematical equations based on photon interaction position and time. These include the sum of two smallest angles between the photons ($\theta_1 + \theta_2$) that are calculated from the interaction positions, energy deposited by a single photon (E_{dep}) in the scintillator, momenta of the most and least energetic photon (k_1, k_3), minimum distance from the detector center to the line of response between every two interactions ($\min d_{\mathrm{LOR}}$), and the time difference between two-photon interactions ($\mathrm{d}t_{ij}$).

The BDT algorithm uses 400 decision trees, each with a maximum depth of 2. The MLP network is configured with 100 training cycles and a single hidden layer containing 10 neurons. The signal and background are split into training and test samples where 50% of the whole sample is used for training and the rest for testing. Picking of training and test samples is done using a random seed. The multivariate techniques in TMVA consider training events for which the desired output is known, *i.e.* either signal or background. It classifies the signal and background events by determining a mapping (response) function that maps the input observable into a single variable for each event [19].

3. Results

The BDT and MLP neural networks evaluation for the considered signal and background classification from training and testing the data set in terms of TMVA response is given in Fig. 1. The distribution at the testing and training stage overlaps shows no over-training effects for each method. The region close to one corresponds to more signal, while the region near zero is dominated by background.

The Receiver Operating Characteristic (ROC) curve representing signal efficiency and background rejection for two different classifiers is given in Fig. 2. There is not much difference in terms of background discriminating powers using the BDT and MLP methods as both curves lie one over the other. The optimal cut value to distinguish signal from background events is decided based on the response of a particular MVA classifier. The value is chosen where the signal efficiency from each MVA classifier is 70%. The events with MVA output greater than the cut value are selected for signal and background events. The exemplary distribution for identified signal and background events is given in Fig. 3 and Fig. 4 for the BDT and MLP classifiers respectively.

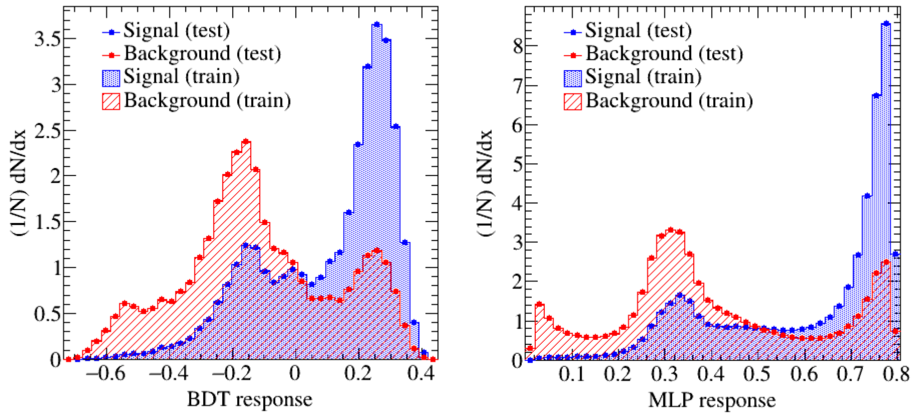

Fig. 1. Normalized distribution of the response from (a) BDT and (b) MLP classifier models for signal and background, shown separately for both the testing and training data. Higher response values reflect the model's confidence in classifying events, with larger values indicating a higher probability of the event being a signal.

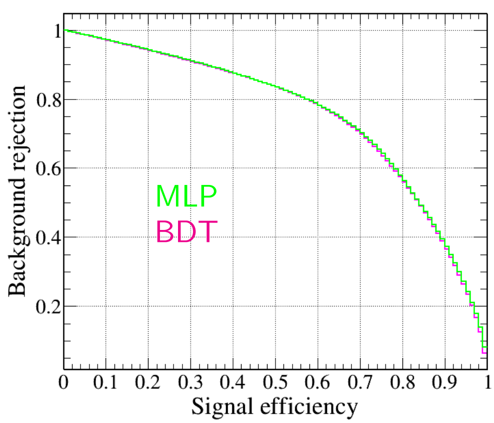

Fig. 2. ROC curve. The distribution for signal efficiency and background rejection after using the BDT (pink) and MLP (green) classifiers to distinguish between the signal and background in the test sample.

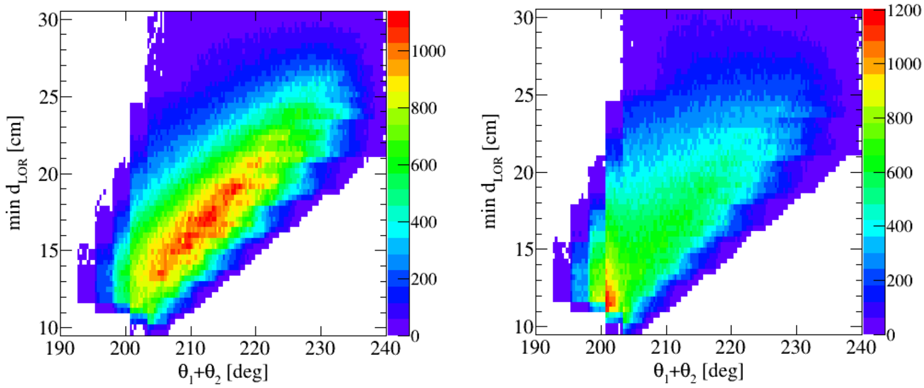

(a) (b)

Fig. 3. Exemplary distribution for signal and background classification from the BDT method using a test MC simulated data sample. The x-axis represents the sum of the two smallest relative angles between the three recorded photons calculated from the center of the detector. The y-axis represents the shortest distance between the hypothetical 2γ annihilation point on the line of response (LOR) to the center of the detector. (a) represents the o-Ps $\to 3\gamma$ events and (b) is for the 3γ background events at the chosen cut value where signal efficiency is 70% for the BDT classifier.

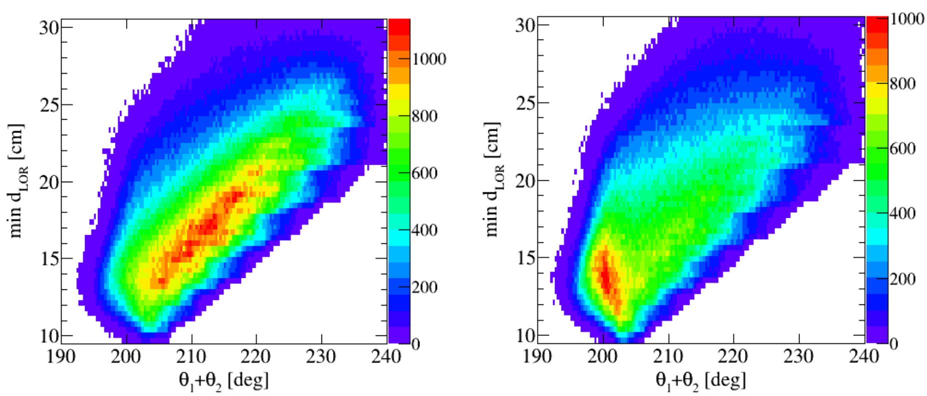

(a) (b)

Fig. 4. The distribution for (a) signal and (b) background events after the threshold value at the signal efficiency of 70% for the MLP method.

4. Conclusion

The multivariate analysis is performed for the identification of signal events via BDT and MLP neural networks. The chosen threshold value is applied to the distribution of a sum of two smallest angles between photons and the minimum distance from the detector center to the line of response (min d_{LOR}) for signal and background events. These algorithms can reject 70% of the background and maintain the signal-to-background ratio to 1.3 in the final sample. The cut-based selection procedure is also performed for the dataset studied in this work, with a similar sequence of cuts on the variables described in Ref. [6]. It is estimated that the signal purity of the data sample is increased from 55% for the cut-based selection method [23] to 70% using multivariate analysis. This approach for event classification would be beneficial with a Modular J-PET detector where we aim to reach the precision of the CPT symmetry test to 10^{-5}.

We acknowledge the support from the National Science Centre (NCN), Poland through grants OPUS 2019/35/B/ST2/03562, MAESTRO 2021/42/A/ST2/00423, and PRELUDIUM 2022/45/N/ST2/04084; SciMat and qLife Priority Research Areas budget under the program Excellence Initiative — Research University at the Jagiellonian University.

REFERENCES

[1] P. Moskal *et al.*, *Acta Phys. Pol. B* **47**, 509 (2016).

[2] W. Bernreuther, U. Low, J.P. Ma, O. Nachtmann, *Z. Phys. C* **41**, 143 (1988).

[3] S.D. Bass, *Acta Phys. Pol. B* **50**, 1319 (2019).

[4] S.D. Bass *et al.*, *Rev. Mod. Phys.* **95**, 021002 (2023).

[5] P.A. Vetter, S.J. Freedman, *Phys. Rev. Lett.* **91**, 263401 (2003).

[6] P. Moskal *et al.*, *Nat. Commun.* **12**, 5658 (2021).

[7] D.W. Jeong *et al.*, *Nucl. Instrum. Methods Phys. Res. A* **989**, 164941 (2021).

[8] C. Bartram, R. Henning, D. Primosch, *Nucl. Instrum. Methods Phys. Res. A* **966**, 163856 (2020).

[9] T.E. Haugen, E.A. George, O. Naviliat-Cuncic, P.A. Voytas, *EPJ Web Conf.* **282**, 01003 (2023).

[10] M.S. Sozzi, *J. Phys. G: Nucl. Part. Phys.* **47**, 013001 (2020).

[11] P. Moskal *et al.*, *Nucl. Instrum. Methods Phys. Res. A* **764**, 317 (2014).

[12] S. Niedźwiecki *et al.*, *Acta Phys. Pol. B* **48**, 1567 (2017).

[13] P. Moskal *et al.*, *Nat. Commun.* **15**, 78 (2024).

[14] P. Moskal *et al.*, *Sci. Adv.* **7**, eabh4394 (2021).

[15] P. Moskal, E.Ł. Stępień, *PET Clin.* **15**, 439 (2020).

[16] P. Moskal *et al.*, *Sci. Adv.* **10**, eadp2840 (2024).

[17] F. Tayefi Ardebili, S. Niedźwiecki, P. Moskal, *Bio-Algorithms Med-Systems* **19**, 132 (2023).

[18] M. Das *et al.*, *Bio-Algorithms Med-Systems* **19**, 87 (2023).

[19] A. Hoecker *et al.*, arXiv:physics.data-an/0703039.

[20] J. Therhaag, *AIP Conf. Proc.* **1504**, 1013 (2009).

[21] https://github.com/JPETTomography/J-PET-geant4

[22] P. Moskal *et al.*, *Nucl. Instrum. Methods Phys. Res. A* **775**, 54 (2015).

[23] J-PET Collaboration (N. Chug), *PoS* **(EPS-HEP2023)**, 366 (2024).